Structural Engineering and Mechanics, *Vol. 68, No. 6 (2018) 735-745*
DOI: https://doi.org/10.12989/sem.2018.68.6.735

An improved Big Bang-Big Crunch algorithm for structural damage detection

Zhiyi Yin[1], Jike Liu[1], Weili Luo*[2] and Zhongrong Lu[1]

[1]*Department of Applied Mechanics and Engineering, School of Aeronautics and Astronautics, Sun Yat-sen University, Guangzhou, Guangdong Province, 510006, P.R. China*
[2]*School of Civil Engineering, Guangzhou University, Guangzhou, Guangdong Province, 510006, P.R. China*

(Received September 7, 2018, Revised November 8, 2018, Accepted November 10, 2018)

Abstract. The Big Bang-Big Crunch (BB-BC) algorithm is an effective global optimization technique of swarm intelligence with drawbacks of being easily trapped in local optimal results and of converging slowly. To overcome these shortages, an improved BB-BC algorithm (IBB-BC) is proposed in this paper with taking some measures, such as altering the reduced form of exploding radius and generating multiple mass centers. The accuracy and efficiency of IBB-BC is examined by different types of benchmark test functions. The IBB-BC is utilized for damage detection of a simply supported beam and the European Space Agency structure with an objective function established by structural frequency and modal data. Two damage scenarios are considered: damage only existed in stiffness and damage existed in both stiffness and mass. IBB-BC is also validated by an existing experimental study. Results demonstrated that IBB-BC is not trapped into local optimal results and is able to detect structural damages precisely even under measurement noise.

Keywords: swarm intelligence; BB-BC algorithm; benchmark test function; damage detection; frequency domain

1. Introduction

With the development of science and technology, many structural facilities are becoming large and complex. Damage arises in those structures owing to aggressive environmental conditions, sudden external events and/or unpredictable inner changes of the materials. Structural strength, stiffness and stability are greatly affected by structural damage, and even structural safety accidents probably occur. Therefore, it is of great importance to localize and quantify the structural damage.

Generally, a structure can be represented as a finite element model composed of piecewise distributed parameters in elements, such as mass, stiffness and damping. When damage occurs, the local structural parameters are changed together with natural frequencies, mode shapes and dynamic responses of the whole system. Thus, damages can be identified through monitoring those data, and two kinds of damage detection methods are proposed: frequency-domain methods and time-domain methods. Time-domain methods often use the displacement or acceleration response data for structural damage detection (Ni 2016, Zhang 2017, Li 2017, Ni 2018), which require less sensors and are sensitive to structural damage even a local damage. On the other hand, frequency-domain methods are efficient, low-cost and non-destructive (Fan and Qiao 2011). Frequency and modal data are independent to damping and external excitation. The modeling errors in frequency-domain methods are smaller than those in time-domain methods because damping is difficult to measure and external excitation is unpredictable. Thus, the frequency-domain methods have been widely used in engineering communities.

From a mathematical point of view, the damage identification can be transformed into an optimization problem. For accessing the optimum solution, an objective function is established to be minimized, which is defined by the discrepancies between the measured data and the computed results. Researchers have put forward lots of conventional optimization methods: least-squares estimation, Lagrangian multiplier method, and maximum likelihood method, for example. However, those traditional methods are sensitive to initial values and require the objective function being analytic, which are difficult to be employed in engineering practice. In recent years, numerous swarm intelligence algorithms are utilized for structure damage detection, such as simulated annealing algorithm (SA), genetic algorithm (GA), artificial ant colony algorithm (ABC), artificial bee colony algorithm (BCO), particle swarm optimization (PSO) and fruit fly optimization algorithm (FOA). It has been proved that the swarm intelligence algorithms could overcome the drawbacks of conventional algorithms in term of operability and analyticity, but would usually lead to a local optimal solution. Hence, researchers have done a great deal of work to improve the original swarm intelligence algorithms in order to apply them into structural damage detection. For instance, Mare and Surace (1996) made used of the GA in damage detection of elastic structures; Chou and Ghaboussi (2001) successfully detected the location and extent of the damage of truss structures with the assistance of the GA; Yin *et al*. (2006) presented an improved genetic algorithm to detect damage of frame structures; Huang *et al*. (2012) proposed a structural damage identification method

*Corresponding author, Assistant Professor
E-mail: wlluo@gzhu.edu.cn

ISSN: 1225-4568 (Print), 1598-6217 (Online)

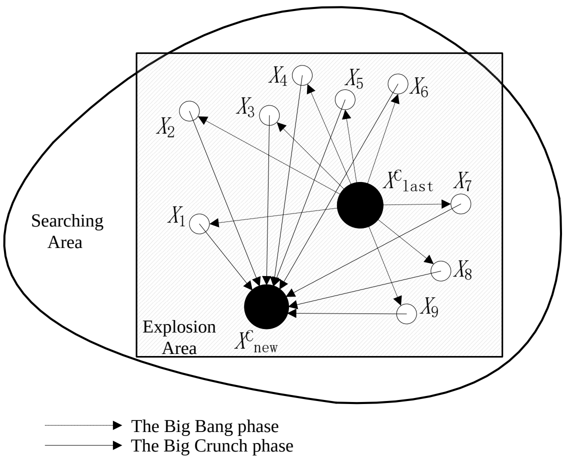

Fig. 1 Schematic diagram of the BB-BC

combining the GA with an improved damage identification factor under noise; Begambrea and Laier (2009) put forward the hybrid PSO-Simplex algorithm according to damage identification procedure using frequency domain data; Kang *et al.* (2012) united the PSO with the artificial immune system and hence presented an immunity enhanced particle swarm optimization algorithm for damage detection of structures; Guo and Li (2014) suggested a two-stage damage identification method, incorporating evidence fusion and the improved particle swarm optimization, in order to solve a structural multi-damage identification problem; Aditi *et al.* (2014) used the continuous ant colony optimization for structural damage detection based on modal parameters; Li and Lu (2015) identified the damage of simply supported beams and trusses using the multi-swarm fruit fly optimization (Yuan e*t al.* 2014); Kaveh and Zolghadr (2015) reported an improved charged system search algorithm to tackle the problem of damage identification of truss structures; Zheng (2018) identified structural damage of beam and plate in time domain using a could model based fruit fly optimization algorithm.

The Big Bang-Big Crunch (BB-BC) algorithm is a new optimization technique of swarm intelligence proposed by Osman and Ibrahim (2006). The original BB-BC converges faster and implements more conveniently compared with the classic GA (Osman and Ibrahim 2006). The BB-BC have been found wide applications in the aspect of construction design optimization: Charles (2007) attempted to put the BB-BC into the use of the design of space trusses; Kaveh and Talatahari (2009) introduced a hybrid Big Bang-Big Crunch optimization algorithm for optimal design of truss structures, and then used the algorithm for the charged system search (Kaveh and Zolghadr 2012); Prayogo *et al.* (2018) presented a differential Big Bang-Big Crunch algorithm for construction-engineering design optimization. However, less attentions have been paid on the application of the BB-BC in damage detection (Zahra *et al.* 2013, Huang and Lu 2017). One possible reason lies in that the original BB-BC is easily trapped into the local optimal solution. The algorithm developed by Zahra *et al.* (2013) can only avoid the local optimal solution in some certain cases because their revisions make candidates as a function the best global solution in all iterations but fail to limit the variation rate. The estimated best global solution would just approximate the real best global solution occasionally based on the inherent property of the BB-BC. Thus, the drawback of the BB-BC has not been completely tackled.

To better prevent local optimization and improve convergence, an improved Big Bang-Big Crunch (IBB-BC) algorithm is put forward in this study for structural damage detection. The performance of IBB-BC has been examined by various unimodal and multimodal benchmark test functions. The IBB-BC is also applied in the damage detection under noise in frequency domain for a simply supported beam structure and a European Space Agency structure. Two damage scenarios have been considered: damage only existed in stiffness and damage existed in both stiffness and mass. An existing experimental study is further used for the validation of the proposed algorithm.

2. The algorithm

2.1 The basic Big Bang-Big Crunch algorithm

The Big Bang-Big Crunch algorithm is based on the Big Bang and Big Crunch theory of the evolution universe. The procedure of the BB-BC is shown in Fig. 1, which is composed of the Big Bang phase and the Big Crunch phase.

In the Big Bang phrase, candidates are generated randomly and disorderly in a searching area from a temporary optimum point (called mass center). The *i*-th candidate $\overrightarrow{X_i}$ is generated by the following distribution rule (Osman and Ibrahim 2006)

$$\vec{X}_i = \vec{X}^{\mathrm{C}} + r\vec{R}(k) \tag{1}$$

where $\vec{X}^{\mathrm{C}}$ is the mass center; *r* is normal distributed random number with a zero mean and a standard deviation of 1; $\vec{R}(k) = \frac{\vec{L}_{\max}-\vec{L}_{\min}}{2} \cdot \frac{1}{k}$ is the radius of the explosion; *k* is the number of iterations; $\vec{L}_{\max}$ and $\vec{L}_{\min}$ are the upper and lower bounds of the search area respectively.

In the Big Crunch phrase, those candidates are drawn into an order and aggregated into a new mass center by gravitation. The position of the new mass center is related to the energy state of each candidate based on the following equation (Osman and Ibrahim 2006)

$$\vec{X}^{\mathrm{C}} = \frac{\sum_{i=1}^{n} \frac{\vec{X}_i}{f_i}}{\sum_{i=1}^{n} \frac{1}{f_i}} \tag{2}$$

where *n* is the number of the candidates; f_i is a fitness value of the *i*-th candidate, which stands for its energy state.

2.2 Improved Big Bang-Big Crunch algorithm

Two drawbacks are found in the basic BB-BC algorithm: (a) it is easy to be trapped into the local optimum because the radius of explosion rapidly reduces with the advance of iteration according to Eq. (1), and (b) randomly generated candidates make mass centers between successive two generations independent, reducing the speed of convergence. To overcome these drawbacks, an improved Big Bang-Big Crunch algorithm (IBB-BC) is proposed in this paper with the following improvements:

To tackle the drawback of local optimum, the function of the radius of explosion is revised as the following equation

$$\vec{R}(k) = \frac{\vec{L}}{2} \cdot \left(1 - \frac{k}{k_{\max}}\right)^2 \tag{3}$$

where $k_{\max}$ is the maximum number of iteration. This revision makes the update of the radius of explosion $\vec{R}(k)$ slower due to the use of a second order function of k in comparison with the inverse proportional function in Eq. (1). This is able to avoid being trapped in the local optimum to the most degree while maintaining fast convergence, and thus improve the accuracy of optimization. It is worth pointing out that the deceleration of the reduction of radius may slow down the convergence. Hence, the following measures are supplemented:

(i) Reduce the standard deviation of the random variable r from 1 to $1/\pi$. The probability for r out of [-1, 1] is less than 0.2%, making more candidates fall into the searching area. In this way, the candidates distribute more concentrated around the temporary optimum point. Thus, the convergence of the algorithm is accelerated.

(ii) Introduce a parameter γ to deal with candidates out of the search area. If $k > \gamma k_{\max}$, $3n$ candidates are generated and n of those in the searching area are selected in the Big Bang phase; while, if $k \le \gamma k_{\max}$, the radius of explosion $\vec{R}(k)$ is chosen as the following equation

$$\vec{R}(k) = \min\left[\vec{X}^{\mathrm{CM}} - \vec{L}_{\min}, \vec{L}_{\max} - \vec{X}^{\mathrm{CM}}, \frac{\vec{L}}{2}\left(1 - \frac{k}{k_{\max}}\right)^2\right] \tag{4}$$

where $\vec{X}^{\mathrm{CM}}$ represents the centroid of the mass centers, which is applied as the temporary optimum point in the next iteration of the IBB-BC. As the iteration increases, the radius of explosion $\vec{R}(k)$ is increasingly reduced according to Eq. (4). By selecting an appropriate value of parameter γ, the reduction of the radius $\vec{R}(k)$ can be properly accelerated after the temporary optimum point approximates the global optimal solution in early iterations. Accordingly, the convergence is enhanced and the appearance of the local optimum can be avoided.

To overcome the second drawback of BB-BC, multiple mass centers (say $m_{\max}$) are generated by repeating the two phases $m_{\max}$ times at each iteration. The centroid of those mass centers is calculated based on the following equation

$$\vec{X}^{\mathrm{CM}} = \frac{\sum_{m=1}^{m_{\max}} \frac{\vec{X}_m^{\mathrm{C}}}{f_m^{\mathrm{C}}}}{\sum_{m=1}^{m_{\max}} \frac{1}{f_m^{\mathrm{C}}}} \tag{5}$$

where $\vec{X}_m^{\mathrm{C}}$ is the m-th mass center, and f_m^{C} is its fitness value. Thus, Eq. (1) is rewritten as follows

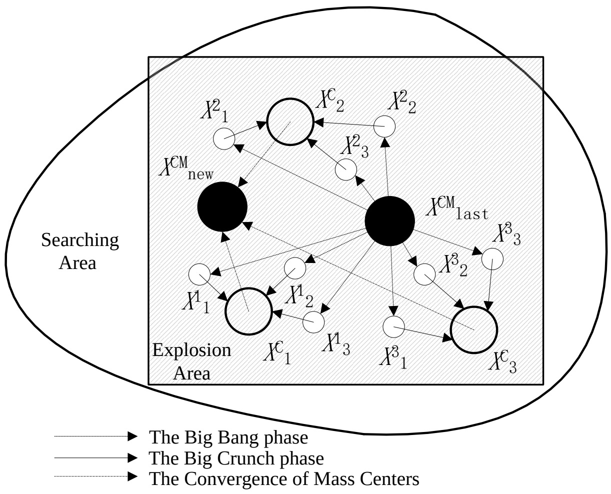

Fig. 2 Schematic diagram of generating multiple mass centers

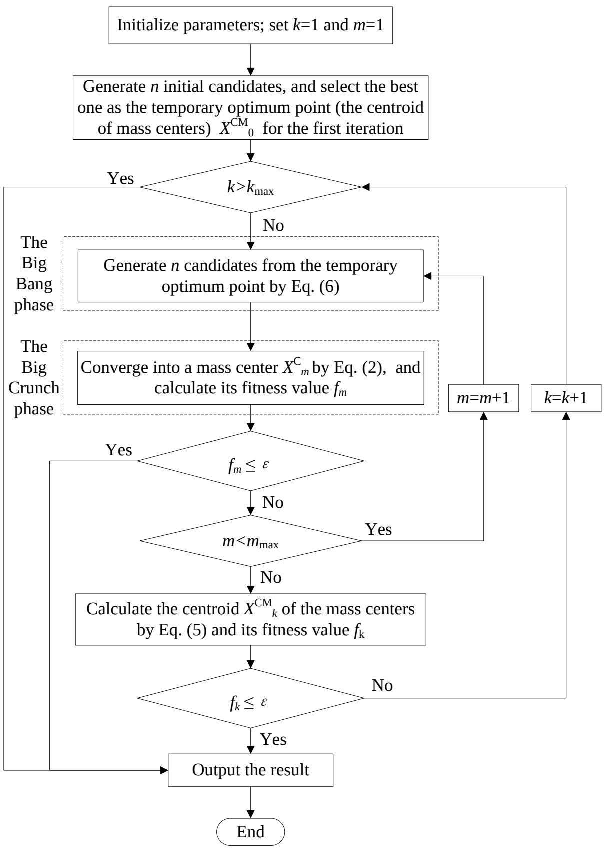

Fig. 3 Flowchart of the IBB-BC

$$\vec{X}_i = \vec{X}^{\mathrm{CM}} + r\vec{R}(k) \tag{6}$$

Fig. 2 illustrates the procedure of generating multiple mass centers. According to Eq. (5), the weighted average of those mass centers determines the temporary optimum point. It will not be stuck even if one of the mass centers jumps into the local optimum, because the others will help the stuck one out of the local optimum. The connection between candidates, mass centers and the temporary optimum point has been strengthened. Furthermore, the location of the temporary optimum point is optimized again

Table 1 List of benchmark test functions

Function name	Equation	Range
Ellipsoid (unimodal)	$F_1 = \sum_{i=1}^{N} i x_i^2$	[-100, 100]
Sphere (unimodal)	$F_2 = \sum_{i=1}^{N} x_i^2$	[-5.12, 5.12]
Step (unimodal)	$F_3 = \sum_{i=1}^{N} (\lvert x_i \rvert + 0.5)^2$	[-10, 10]
Ackley (multimodal)	$F_4 = 20 + \mathrm{e} - 20\mathrm{e}^{-0.2\sqrt{\frac{1}{N}\sum_{i=1}^{N} x_i^2}} - \mathrm{e}^{\frac{1}{N}\sum_{i=1}^{N}\cos(2\pi x_i)}$	[-10, 10]
Rastrigin (multimodal)	$F_5 = 10N + \sum_{i=1}^{N} \left[x_i^2 - 10\cos(2\pi x_i)\right]$	[-5.12, 5.12]
Griewank (multimodal)	$F_6 = 1 + \sum_{i=1}^{N} \frac{x_i^2}{4000} - \prod_{i=1}^{N} \cos\left(\frac{x_i}{\sqrt{i}}\right)$	[-50, 50]

by the convergence of mass centers, which is beneficial for the acceleration of global convergence and the reduction of iteration time.

In the first few iterations, it is unlikely that the temporary point is trapped in the local optimum due to the wide distribution of candidates. In that case, the number of mass centers does not need to be increased. On the contrary, it is more necessary to increase the number of mass centers because the radius of explosion shrinks smaller and candidates are more concentrated as the iteration increases. Hence, the number of mass centers is set to be dependent the time of iteration

$$m_{\max} = \left[NT \cdot \left(\frac{k}{k_{\max}} \right)^{a} \right] \quad (7)$$

where NT is the maximum number of mass centers in the whole calculation; a is a parameter to limit the rate of the change, which is generally within the range (0, 6].

3. Implementations

The flowchart of the IBB-BC is shown in Fig. 3 with main steps described as follows:

Step 1. Initialize parameters of the IBB-BC, such as n, $k_{\max}$, NT, a, γ, and set $k = 1$, $m = 1$;

Step 2. Produce initial n candidates randomly in the searching area and calculate their fitness values, and choose the best candidate as the first temporary optimum point;

Step 3. Generate n candidates in a random manner from the temporary optimum point by Eq. (6);

Step 4. Calculate the fitness values of the candidates, and astringe them to a mass center $\vec{X}_m^{\mathrm{C}}$ by Eq. (2);

Step 5. Calculate fitness value f_m of the mass center. If it satisfies a stop criterion ($f_m \leq \varepsilon$), the algorithm is terminated and the current mass center is output as the global optimal solution. Otherwise, set $m = m + 1$ and return to Step 3 till $m > m_{\max}$;

Step 6. Calculate the centroid $\vec{X}^{\mathrm{CM}}$ of those mass centers $\vec{X}_m^{\mathrm{C}}$ (m = 1, 2…, $m_{\max}$) by Eq. (5) and the fitness value of $\vec{X}^{\mathrm{CM}}$. The computation stops if a criterion ($f_k \leq \varepsilon$) is satisfied, and the current $\vec{X}^{\mathrm{CM}}$ is output as the global optimal solution. On the contrary, the current $\vec{X}^{\mathrm{CM}}$ is regarded as the temporary optimum point. In this case, set $k = k + 1$ and $m = 1$, and then return to Step 3 till $k > k_{\max}$.

4. Benchmark tests

The IBB-BC is tested and compared with the BB-BC by several benchmark problems listed in Table 1, including Ellipsoid, Sphere, Step, Ackley, Rastrigin and Griewank functions (Osman and Ibrahim 2006, Jordehi 2014). These functions can be classified into two categories: unimodal functions and multimodal functions.

The dimension N is equal to either 2 or 10 for both six functions. The number of candidates n is uniformly set as 40 and parameters γ and a are chosen to be 0.2 and 3 respectively. For the purpose of economizing computational resource, the maximum of iteration $k_{\max}$ and the maximum number of mass centers NT are set differently according to the different properties of those functions, which is given as follows: when $N = 2$, $k_{\max}$ from F_1 to F_6 are successively chosen to be 30, 30, 800, 200, 30 and 50 respectively, and NT is equal to 2 for all the six functions; when $N = 10$, $k_{\max}$ from F_1 to F_6 are selected to be 500, 50, 800, 1000, 2000 and 1000 respectively, and NT are equal to 12, 12, 20, 12, 50 and 30 respectively. Each test is carried out for 100 independent trails and the average of the optimal solutions is taken for the comparison with actual values directly calculated by the functions. For describing the accuracy of results conveniently, the following function is introduced as a performance measure

$$\Delta F_i = \lvert F_i - F_{\mathrm{a}i} \rvert \quad (8)$$

where F_i is the calculated value of the i-th function by IBB-BC or BB-BC, and $F_{\mathrm{a}i}$ is its actual value. If $\Delta F_i < 10^{-5}$ is satisfied, the calculation stops and the corresponding result is an output as the optimal solution.

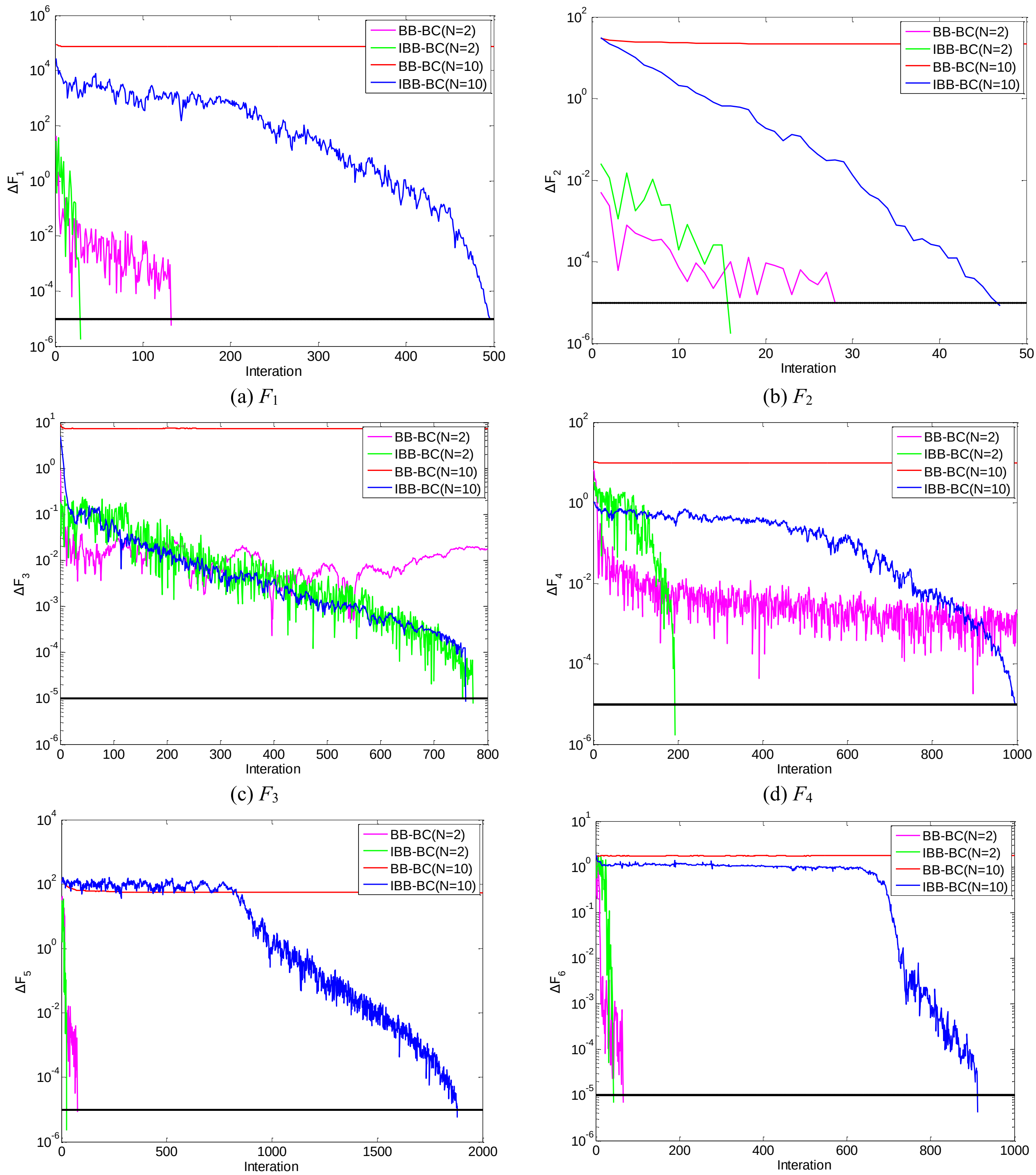

(a) F_1 (b) F_2

(c) F_3 (d) F_4

(e) F_5 (f) F_6

Fig. 4 Comparison of the convergence results of the IBB-BC with the BB-BC on various benchmark test functions

Fig. 4 shows a comparison of the convergence of the six benchmark test functions between the IBB-BC and the BB-BC. When the dimension N is 2, the iteration numbers of the IBB-BC are 29, 16, 26, 42 for Ellipsoid function F_1 (Fig. 4(a)), Sphere function F_2 (Fig. 4(b)), Rastrigin function F_5 (Fig. 4(e)), and Griewank function F_6 (Fig. 4(f)), respectively; while the iteration numbers are much larger for BB-BC, which are 132, 28, 76, 66, respectively. Figs. 4(c) and 4(d) show, under the condition of $N = 2$, that BB-BC makes Step function F_3 and Rastrigin function F_4 having the tendency to converge but fail to obtain accurate results; in contrast, IBB-BC is still able to obtain optimal solution within the given maximal iteration number. It is worth mentioning that BB-BC not always successfully obtains the optimal solution for multimodal functions among 100 independent trails, while IBB-BC works for all

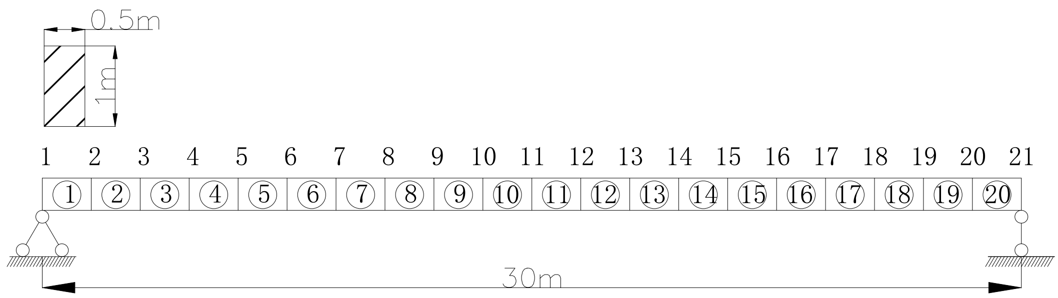

Fig. 5 Finite element model of a simply supported beam with 20 elements

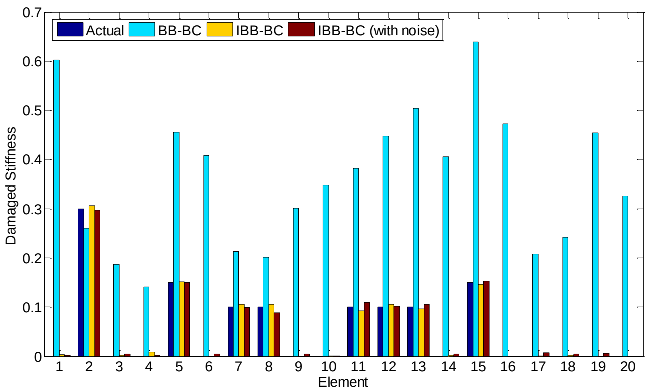

Fig. 6 Bar chart of the detection of the Simply Supported Beam with damage existed in stiffness only

trails. When the dimension *N* is equal to 10, BB-BC fails to converge to the optimal solution for all the six functions, however, IBB-BC always does. This reveals that IBB-BC is applicable for functions with high dimension, and BB-BC no longer works.

As a summary, the Benchmark tests show that IBB-BC is more efficient, effective and accurate than BB-BC, regardless of unimodal functions and multimodal functions in either low or high dimension.

5. Structural damage detection using improved Big Bang-Big Crunch algorithm

Both IBB-BC and BB-BC are employed for the damage detection of a simply supported beam and the European Space Agency structure respectively. The objective function is defined as a function of the natural frequencies and mode shapes of the structures.

5.1 Parameterization of structural damage

A general finite element model for a linear elastic structural dynamic system without damping can be described as the problem of generalized eigenvalue as the following equation

$$(\boldsymbol{K} - \omega_i^2 \boldsymbol{M})\boldsymbol{\Phi}_i = 0 \tag{9}$$

where $\boldsymbol{K}$ and $\boldsymbol{M}$ are the stiffness matrix and the mass matrix of the finite system respectively; ω_i and $\boldsymbol{\Phi}_i$ are the i-th order nature frequency and mode shape respectively. For describing the damage of structure, parameters α and β (called damage coefficients) are introduced to represent the decrease of stiffness and mass respectively. The relationship between the stiffness and the mass matrixes and the damage coefficients are illustrated as the following equation

$$\begin{cases} \boldsymbol{K} = \sum_{j=1}^{n_e} (1-\alpha_j) k_j^e \\ \boldsymbol{M} = \sum_{j=1}^{n_e} (1-\beta_j) m_j^e \end{cases} \tag{10}$$

where n_e is the number of elements; k_j^e and m_j^e are the stiffness and the mass matrixes of the j-th element respectively; α_j and β_j are the damage coefficient of stiffness and mass for the j-th element respectively, and $0 \le \alpha_j,\ \beta_j \le 1$. If the element is completely destroyed in stiffness, the stiffness coefficient α_j is equal to 1; α_j is equal to 0 in the case where the element remains intact. Similarly, β_j is defined as the values of 1 and 0 indicating a complete loss of mass and no loss at all, respectively.

An objective function is established as the following equation based on frequency residue and modal assurance criteria (Kang *et al*. 2012)

$$\begin{cases} f = \sum_{i=1}^{NF} [w_{\omega i}^2 \Delta\omega_i^2 + w_{\boldsymbol{\Phi} i}^2 (1 - MAC_i)] \\ \Delta\omega_i = \dfrac{|\omega_i^C - \omega_i^M|}{|\omega_i^M|} \\ MAC_i = \dfrac{(\boldsymbol{\Phi}_i^C \cdot \boldsymbol{\Phi}_i^M)^2}{\|\boldsymbol{\Phi}_i^C\|^2 \|\boldsymbol{\Phi}_i^M\|^2} \end{cases} \tag{11}$$

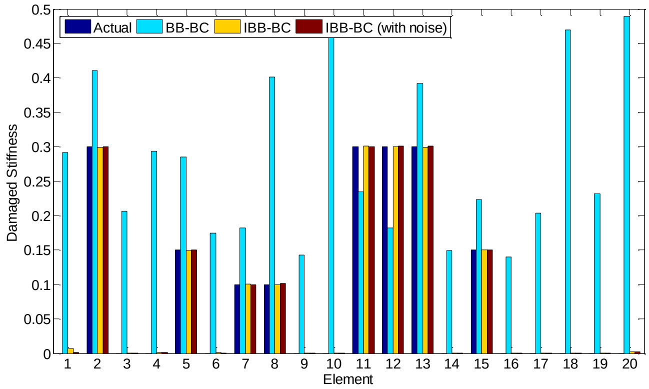

(a) Result of stiffness

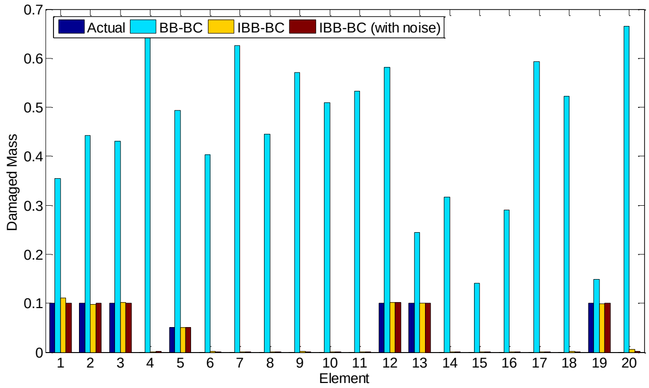

(b) Result of mass

Fig. 7 Bar chart of the detection of the simply supported beam with damage existed in both stiffness and mass

where ω_i^{C} and $\boldsymbol{\Phi}_i^{\mathrm{C}}$ are the i-th order calculated frequency and modal shape respectively; ω_i^{M} and $\boldsymbol{\Phi}_i^{\mathrm{M}}$ are the i-th order measured frequency and mode shape respectively; $w_{\omega i}$ and $w_{\boldsymbol{\Phi} i}$ are the corresponding weight coefficients; *NF* is the number of orders selected for calculation.

In practice, the environmental noise has a great influence on the detection of damage. Herein, the effect of artificial noise in damage detection is introduced as the following equation in the simulation (Mak 2001).

$$\begin{cases} \omega_i' = \omega_i(1+\rho_\omega r_i) \\ \boldsymbol{\Phi}_i' = \boldsymbol{\Phi}_i(1+\rho_{\boldsymbol{\Phi}} r_i) \end{cases} \tag{12}$$

where ω_i' and $\boldsymbol{\Phi}_i'$ are the i-th order natural frequency and mode shape affected by noise; ρ_ω and $\rho_{\boldsymbol{\Phi}}$ are the noise level for the natural frequency and mode shape; r_i is a random variable subjected to the normal distribution.

5.2 Numerical examples

5.2.1 A simply supported beam

A simply supported beam with 20 elements is applied in damage detection in this section. Fig. 5 shows its finite model with 21 nodes and 20 elements. The density of the material is 2800 kg/m^3 and the Young's modulus is 3.4×10^{10} N/m^2. Two damage cases are considered: one assumes the damage existed in stiffness only, and the other assumes both stiffness and mass having damages.

Case 1. Damage existed in stiffness only

In this case, it is assumed that the damage of the structure only causes the decrease of stiffness, and the mass remains intact, that is, $\beta_j = 0$ $(j = 1,2,3,\ldots,n_{\mathrm{e}})$.

The assumed damage conditions and the results of simulation are exhibited in Fig. 6. Elements 2, 5, 7, 8, 11, 12, 13 and 15 are assumed to be damage with various degrees of the reductions of stiffness respectively. The number of candidates n in each Big Bang phase, the maximum of iteration $k_{\max}$ and the maximum number of mass centers *NT* are chosen to be 50, 5000 and 2 respectively. Parameter γ is set as 0.2 and a is 2. The first six natural frequencies and mode shapes of the whole deflection are selected for the objective function (Eq. (11)), and their noise levels are 1.0% and 10% respectively.

Fig. 6 shows that IBB-BC can detect the location of damage, while BB-BC gives many false identifications. The extent of the damage can be identified accurately by IBB-BC with the maximum relative error between the actual data and the identified data less than 0.9%. Even in the influence of the artificial noise, the relative error is within 1.3%. These show that IBB-BC is effective and accurate to the structure damage detection and insensitive to noise.

Case 2. Damage existed in stiffness and mass

It is assumed that the damage of the structure leads to the decrease both in the stiffness and mass at the same time. In this case, the number of damage parameters to be identified is two times of that in Case 1. Besides, Eq. (10) is more difficult to solve due to the coupling of damage parameters.

The damage elements in stiffness are the same as that in

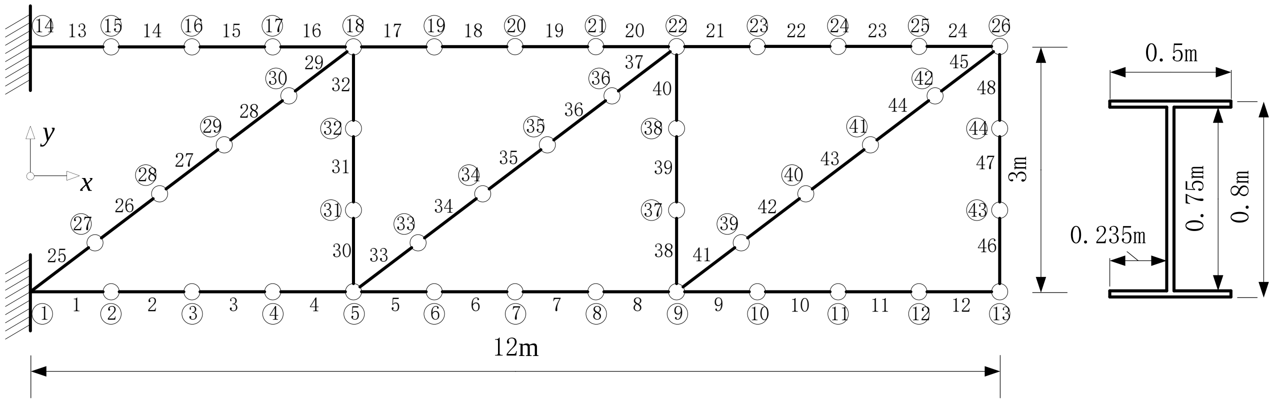

Fig. 8 Finite element model of the the European Space Agency structure

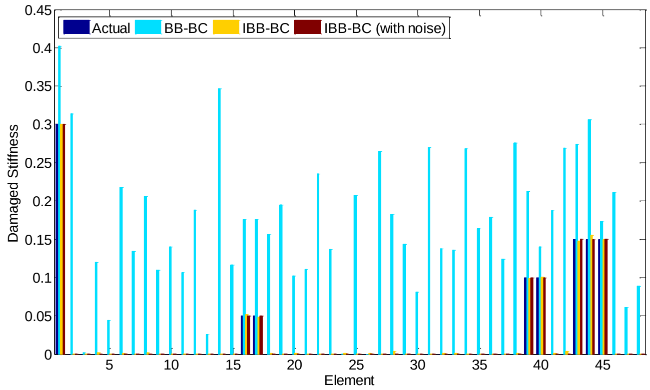

Fig. 9 Bar chart of the detection of the European Space Agency structure with damage existed in stiffness only

Case 1, and damages in mass are extra introduced in elements 1, 2, 3, 5, 12, 13 and 19 with amplitude varying from 0.05 to 0.1 times their corresponding elementary masses. For practice, the damages in mass are two times less than that in stiffness in the same element. Parameters of IBB-BC and BB-BC are equal to that in Case 1 except that the maximum number of mass centers NT is increased to 3. The first ten natural frequencies and mode shapes of the whole deflection are chosen for the calculation of the objective function.

As shown in Fig. 7, BB-BC cannot detect the damage of the structure, and IBB-BC successfully identifies the location and extent of structural damage. The maximum relative error of the results without the influence of noise is 1.12%. The error of the results with noise is within 0.53%. These show the accuracy of IBB-BC for damage detection and its insensitivity of noise. It is also confirmed that IBB-BC is applicable to the case of detecting the structure damage existed in both stiffness and mass.

5.2.2 The European Space Agency structure

The European Space Agency structure studied in this section is shown in Fig. 8. It is divided by 44 nodes and connected by 48 frame elements. Each node has 3 dofs, resulting in a total of 132 dofs in the structure. The density of the material is 2800 kg/m^3 and the Young's modulus is 7.5×10^{10} N/m^2. Similar to the previous example, two cases are considered with one having damage in stiffness and the other in both stiffness and mass.

Case 1. Damage existed in stiffness only

The structure damage only exists in stiffness in this case. The assumed damage conditions and the results of simulation are exhibited in Fig. 9. Elements 1, 16, 17, 39, 40, 43, 44 and 45 are assumed to have certain degrees of damage in stiffness varying from 5% to 30%. These elements cover most of possible damaged elements in the structure, among them element 1 and elements 16 and 17 are adjacent to the joints of the truss structure, elements 39 and 40 are in a vertical member, and the rest of elements are in a diagonal member. The number of candidates n, the maximum of iteration $k_{\max}$ and the maximum number of mass centers NT are equal to 50, 8000 and 3 respectively. Parameter γ is 0.2, and a is 1. The first eighteen natural frequencies and mode shapes of the whole displacement in y direction are selected for the objective function (Eq. (12)), and their noise levels are 1.0% and 10% respectively.

Fig. 9 shows that IBB-BC can identify the structural damage precisely with maximum errors less than 6.1% without noise and 6.0% with noise. The BB-BC is not effective for the detection on the contrary. Although the number of dofs of the European Space Agency structure is larger than the simply supported beam in Section 5.2.1, and the IBB-BC is still practicable and accurate for the damage detection and not sensitive to noise.

Case 2. Damage existed in stiffness and mass

In this case, both BB-BC and IBB-BC are compared in terms of accuracy and noise-sensitivity in the damage detection of the European Space Agency structure when the

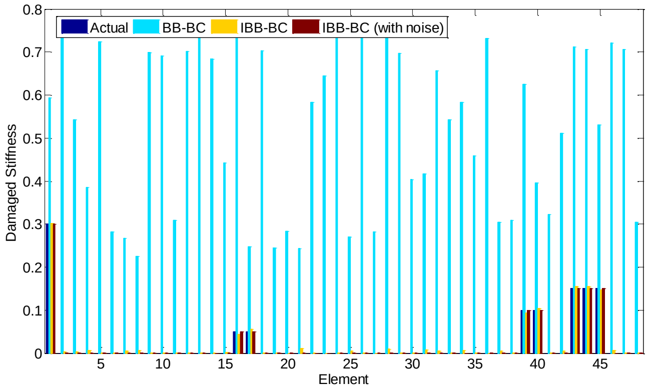

(a) Result of stiffness

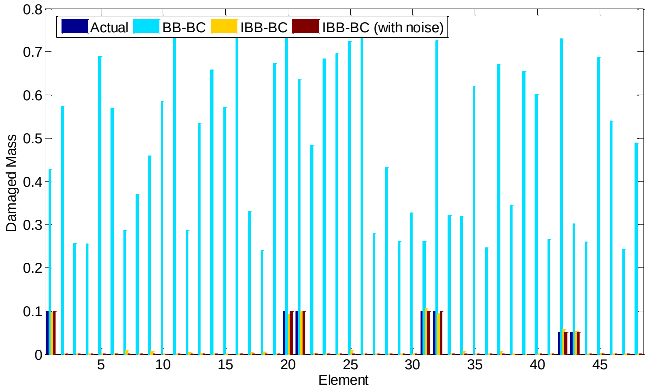

(b) Result of mass

Fig. 10 Bar chart of the detection of the European Space Agency structure with damage existed in both stiffness and mass

stiffness and mass damage occur simultaneously. Similar damages in stiffness are set as the same as Case 1, and damages in mass are extra introduced to elements 1, 20, 21, 31, 32, 42 and 43. The maximum of iteration $k_{\max}$ and the maximum number of mass centers NT are increased to 12000 and 12 respectively in Case 2, and other parameters of IBB-BC and BB-BC are the same as that in Case 1. The first thirty-one natural frequencies and mode shapes of the whole displacement in y direction are chosen for the calculation of the objective function.

Fig. 10 shows that a great discrepancy of the actual value can be found in the results of BB-BC, while the results of IBB-BC are rather promising with a maximal error of 1.09%. Being consistent with previous observations, the influence of noise induces less than 0.10% error which is neglectable.

5.2.3 Discussions

The BB-BC and IBB-BC are employed in the damage detection of simply supported beam and the European Space Agency structure. Two conditions are considered: damages only exist in stiffness and damages exist in both mass and stiffness. The BB-BC is trapped into the local optimal solution as the radius of explosion reduces rapidly. This also renders BB-BC to converge to the optimal solution nearby the initial candidate, instead of the global optimal solution. Thus, all results of BB-BC are far away from the actual results. However, the improvements in IBB-BC overcome the inherent shortcomings of BB-BC. The IBB-BC can accurately detect the locations and extent of the structural damages in mass or/and stiffness. The error between the actual results and that of IBB-BC is minor. In addition, IBB-BC is insensitive to the artificial noise.

6. Experimental validation

An experimental cantilever beam in the reference (Hjelmstad and Shin 1996) is considered to validate the effectiveness of IBB-BC for structural damage detection. Fig. 11 shows the finite model of the experimental beam where a single crack is in Element 5. Because the height-to-length ratio of the beam is 1/15 greater than 1/20, the shear effect is considered and the beam is model by Timoshenko beam elements. The material properties are that density ρ = 7800 kg/m^3, Young's modulus E = 206 GPa and Poisson's ratio ν = 0.3. The first three frequency of the damaged experimental beam can be extracted from the reference (Hjelmstad and Shin 1996), and they are measured as 171, 987 and 3034 Hz respectively. The parameter of the IBB-BC is set as follows: the number of candidates n = 50, the maximum of iteration $k_{\max}$ = 3000 and the maximum number of mass centers NT = 3. Parameter γ is 0.2, and a is 2. The damage of the beam is caused by the crack in Element 5. Thus, it is supposed that the damage only generates the decrease of stiffness of Element 5.

The results of the experimental cantilever beam using both BB-BC and IBB-BC are displayed in Fig. 12. For IBB-

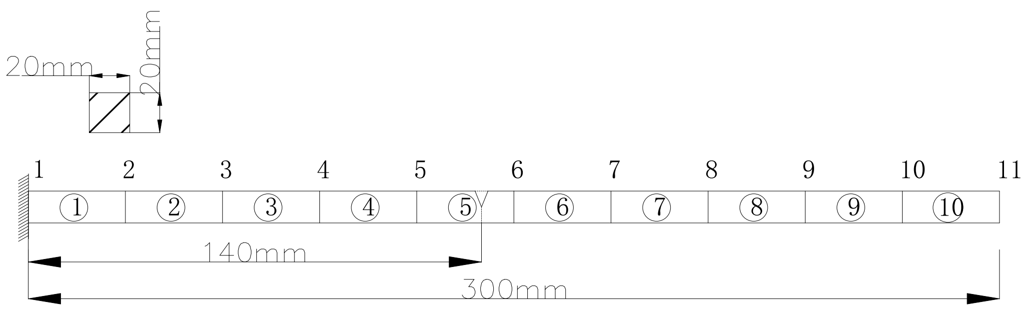

Fig. 11 Finite element model of the cracked cantilever beam

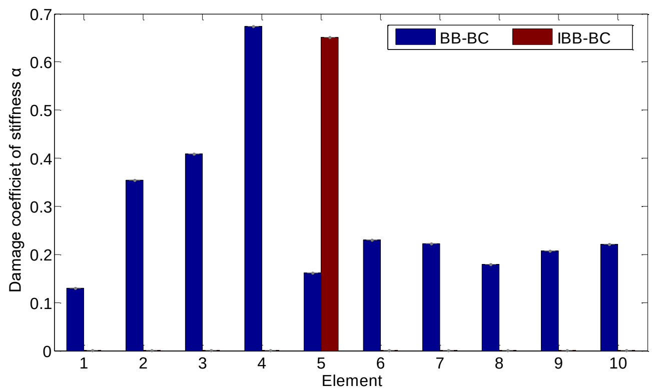

Fig. 12 Damage detection result of the experimental cantilever beam using the BB-BC and the IBB-BC

BC, the damage coefficient of stiffness of Element 5 $\alpha_5 = 0.6507$ and that of other elements is equal to almost zero, perfectly agreeing with the true experimental damage. However, the location and extent of structural damage cannot be detected using BB-BC.

7. Conclusions

An improved Big Bang-Big Crunch algorithm was proposed in this study. Two improvements have been introduced: one is to prevent the local optimum, and the other is to increase the speed of convergence. The improved algorithm performs more applicably, efficiently and accurately compared with the original one. The locations and extents of various structure damages can be detected accurately in the structures studied in this paper by employing the improved Big Bang-Big Crunch algorithm. The improved algorithm shows its insensitivity of noise and its good capacity for engineering practice.

Acknowledgments

This work is supported by the National Key Research and Development Program of China (project No. 2017YFC1500400), National Natural Science Foundation of China (51808147, 11572356), Science and Technology Planning Project of Guangdong Province (2016A020223006) and the Fundamental Research Funds for the Central Universities (17lgjc42).

References

Begambrea, O. and Laier, J.E. (2009), "A hybrid particleswarm optimization-simplex algorithm (PSOS) for structural damage identification", *Adv. Eng. Softw.*, **40**(9), 883-891

Charles, V.C. (2007), "Design of space trusses using Big Bang-Big Crunch optimization", *J. Struct. Eng.*, **133**(7), 999-1008.

Chou, J.H. and Ghaboussi, J. (2001), "Genetic algorithm in structural damage detection", *Comput. Struct.*, **79**(14), 1335-1353.

Fan, W. and Qiao, P. (2011), "Vibration-based damage identification method: A review and comparative study", *Struct. Health Monitor.*, **13**(4), 430-444.

Guo, H.Y. and Li, Z.L. (2014), "Structural damage identification based on evidence fusion and improved particle swarm optimization", *J. Vibr. Contr.*, **20**(9), 1279-1292.

Hjelmstad, K.D. and Shin, S. (1996), "Crack identification in a cantilever beam from modal response", *J. Sound Vibr.*, **198**(5), 527-545.

Huang, J.L. and Zhong, R.L. (2017), "BB-BC optimization algorithm for structural damage detection using measured acceleration responses", *Struct. Eng. Mech.*, **64**(3), 353-360.

Huang, M.S., Wu, L. and Zhu, H.P. (2012), "Structural damage identification based on improved damage identification factor and genetic algorithm under noise", *J. Vibr. Shock*, **31**(21), 168-174.

Kang, F., Li, J. and Xu, Q. (2012), "Damage detection based on improved particle swarm optimization using vibration data", *Appl. Soft Comput.*, **12**(8), 2329-2335.

Kaveh, A. and Talatahari, S. (2009), "Size optimization of space trusses using Big Bang-Big Crunch algorithm", *Comput. Struct.*, **87**(17-18), 1129-1140.

Kaveh, A. and Zolghadr, A. (2012), "Truss optimization with natural frequency constraints using a hybridized CSS-BBBC algorithm with trap recognition capability", *Comput. Struct.*,

102, 14-27.
Kaveh, A. and Zolghadr, A. (2015), "An improved CSS for damage detection of truss structures using changes in natural frequencies and mode shapes", *Adv. Eng. Softw.*, **80**, 93-100.
Li, J., Hao, H. and Chen, Z.W. (2017), "Damage identification and optimal sensor placement for structures under unknown traffic-induced vibrations", *J. Aerosp. Eng.*, **30**(2), B4015001.
Li, S. and Lu, Z.R. (2015), "Multi-swarm fruit fly optimization algorithm for structural damage identification", *Struct. Eng. Mech.*, **56**(3), 409-422.
Majumdar, A., Nanda, B., Malti, D.K. and Maity, D. (2014), "Structural damage detection based on modal parameters using continuous ant colony optimization", *Adv. Civil Eng.*, 1-14.
Mares, C. and Surace, C. (1996), "An application of genetic algorithm to identify damage in elastic structures", *J. Sound Vibr.*, **195**(2), 195-215.
Ni, P. and Law, S. (2016), "Hybrid computational strategy for structural damage detection with short-term monitoring data", *Mech. Syst. Sign. Proc.*, **70**, 650-663.
Ni, P., Xia, Y., Li, J. and Hao, H. (2018), "Improved decentralized structural identification with output-only measurements", *Measure.*, **122**, 597-610.
Osman, K.E. and Ibrahim, E. (2006), "A new optimization method: Big Bang-Big Crunch", *Adv. Eng. Softw.*, **37**(2), 106-111.
Prayogoa, D., Cheng, M.Y., Wu, Y.W., Herdany, A.A. and Prayogo, H. (2018), "Differential Big Bang-Big Crunch algorithm for construction-engineering design optimization", *Automat. Constr.*, **85**, 290-304.
Rezaee Jordehi, A. (2014), "A chaotic-based big bang-big crunch algorithm for solving global optimization problems", *Netur. Comput. Appl.*, **25**(6), 1329-1335.
Shan, M.P. (2001). "Incomplete dynamic measurement in structural damage assessment", M.Sc. Dissertation, Hong Kong Polytechnic University, Hong Kong.
Tabrizian, Z., Afshari, E., Amiri, G.G., Beigy, A., Hossein, M. and Nejad, S.M.P. (2013), "A new damage detection method: Big Bang-Big Crunch (BB-BC) algorithm", *Shock Vibr.*, **20**(4), 633-648.
Tao, Y., Zhu, H.P. and Yu, L. (2006), "Application study of an improved genetic algorithm for frame structure damage detection", *J. Vibr. Eng.*, **19**(4), 525-531.
Yuan, X., Dai, X., Zhao, J. and He, Q. (2014), "On a novel multi-swarm fruit fly optimization algorithm and its application", *Appl. Math. Comput.*, **233**, 260-271.
Zhang, W., Li, J., Hao, H. and Ma, H.W. (2017), "Damage detection in bridge structures under moving loads with phase trajectory change of multi-type vibration measurements", *Mech. Syst. Sign. Proc.*, **87**, 410-425.
Zheng, T., Liu, J., Luo, W. and Lu, Z. (2018), "Structural damage identification using cloud model based fruit fly optimization algorithm", *Struct. Eng. Mech.*, **67**(3), 245-254.

CC